PADI4 minor haplotype as risk factor for excessive NET formation and associated wound healing disorders in diabetes mellitus

Sabrina Ehnert,[1,*] Philipp Hemmann,[1] Christoph Ihle,[1] Caren Linnemann,[1] Jonas Mück,[1] Panagiota-Georgia Anastasiou,[1,2] Ralf Lobmann,[2] Gunnar Blumenstock,[3] Stefan Pscherer[1,4] Andreas Fritsche,[5] Heiko Baumgartner,[1] Tina Histing,[1] Mika F. Rollmann,[1] Andreas K. Nussler[1]

[1] Siegfried Weller Research Institute; BG Unfallklinik Tübingen; Department of Trauma and Reconstructive Surgery; University of Tübingen; Schnarrenbergstr. 95; D-72076 Tübingen; Germany;

[2] Clinic for Endocrinology; Diabetology and Geriatric Medicine; Center for Internal Medicine; Klinikum der Landeshauptstadt Stuttgart gKAöR, Katharinenhospital; Kriegsbergstrasse 60, D-70174 Stuttgart; Germany;

[3] Institute for Clinical Epidemiology and Applied Biometry; University of Tübingen; Silcherstr. 5; D-72076 Tübingen; Germany;

[4] Department of Internal Medicine III, Sophien- and Hufeland-Hospital, Henry-van-de-Velde-Straße 2, D-99425 Weimar, Germany;

[5] Department of Internal Medicine, Division of Diabetology, Endocrinology, and Nephrology, Eberhard Karls University Tübingen, Otfried-Müller-Straße 10, D-72076 Tübingen, Germany

Corresponding author: Sabrina Ehnert, Siegfried Weller Research Institute; BG Unfallklinik Tübingen; Department of Trauma and Reconstructive Surgery; University of Tübingen; Schnarrenbergstr. 95; D-72076 Tübingen; Germany; Tel: +49 (0)7071 606 1065; Email: Sabrina.Ehnert@med.uni-tuebingen.de & Sabrina.Ehnert@gmail.com

Conflict-of-interest statement: The authors have declared that no conflict of interest exists. Parts of the data presented were obtained during the doctoral thesis work of C.L., J.M., and P.-G.A.

Abstract

Diabetes mellitus (DM) is associated with impaired wound healing, partly driven by excessive neutrophil extracellular trap (NET) formation mediated by peptidyl-arginine deiminase 4 (PADI4). While circulating NET markers predict poor healing outcomes, they likely reflect established tissue damage and offer limited opportunity for early intervention. We therefore investigated the association between PADI4 haplotypes, PADI4 expression, NET formation, and clinical outcomes, namely infections and delayed wound and bone healing, in 687 surgical patients (44.7% with DM). Pre-surgical PADI4 expression was 9.4-fold higher in patients with DM, particularly in those who developed wound healing complications. Neutrophils carrying the PADI4 minor haplotype showed increased PADI4 mRNA and protein expression and produced larger quantities of NETs more rapidly than those with the major haplotype. Clinically, patients with DM carrying the minor haplotype had the highest rates of delayed wound healing and infections. Together, these results demonstrate that PADI4 genetic variation influences neutrophil behavior and clinical outcomes. PADI4 haplotyping may provide a clinically actionable biomarker to identify patients with DM at high risk for wound healing complications and guide early preventive strategies.

Funding This study received funding from the German Research Council (EH471/5-1) and the Bundesministerium für Bildung und Forschung (13GW0661D). C.L. was supported by the Studienstiftung des deutschen Volkes.

Keywords Diabetes, Wound Healing, Tissue Infection, Neutrophil Extracellular Traps, PADI4 haplotype

49 **Graphical Abstract**

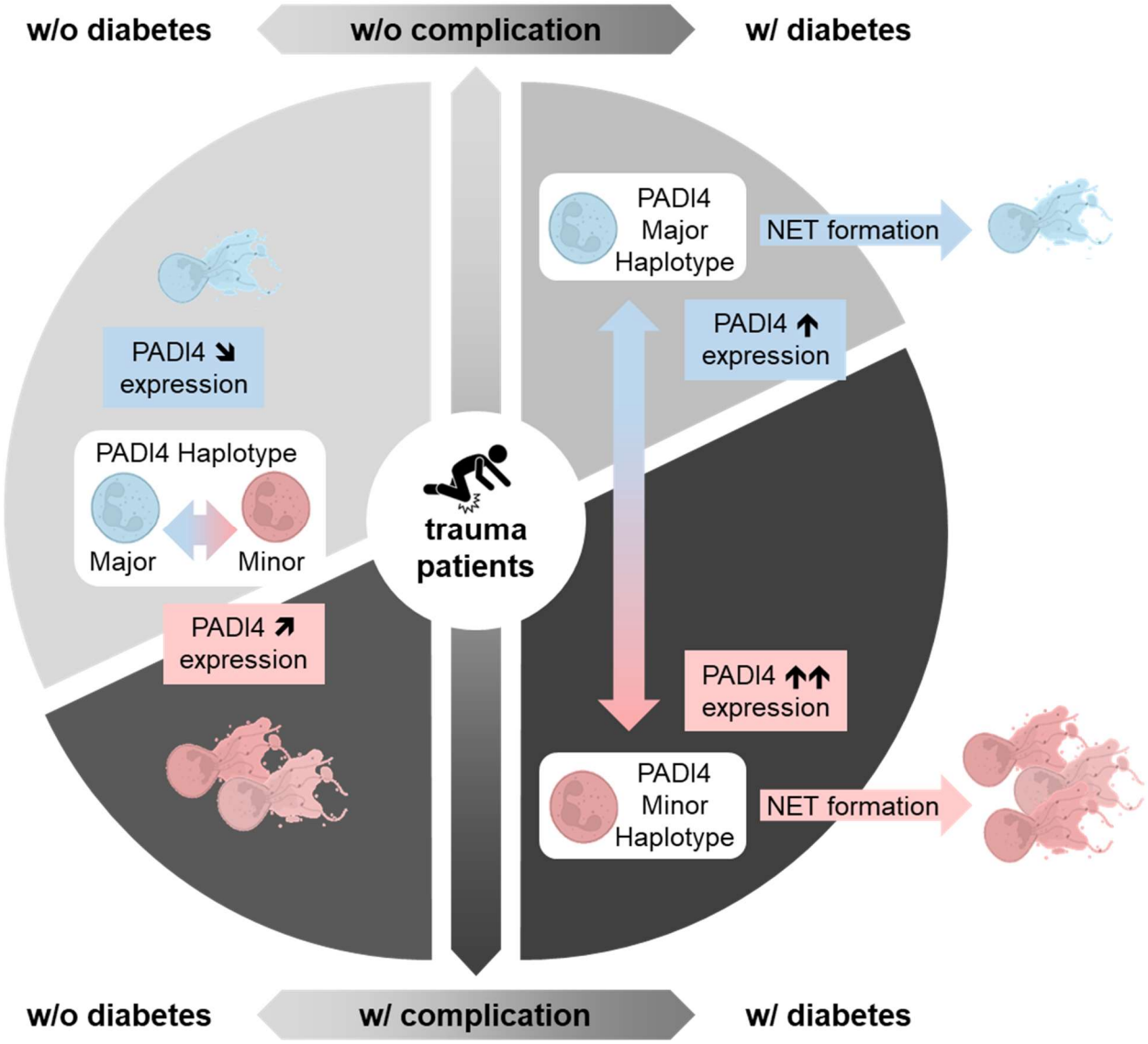

50

51

52 ## Introduction

53 A constantly aging society and sedentary lifestyle made Diabetes mellitus (DM), especially DM
54 type 2, the disease with the fastest growing incidence and prevalence worldwide. Based on
55 reports from the world health organization, DM is a major cause of blindness, kidney failure, heart
56 attacks, or stroke. Likewise, it is indisputable that DM affects the quality of bones and surrounding
57 soft tissues, increasing the risk of fractures and associated healing disorders, *e.g.*, infections
58 and/or delayed bone and wound healing. Approximately every tenth develops a foot ulcer, diabetic
59 foot syndrome, or charcot-osteoarthropathy within the first 5 years of the disease. Of these
60 roughly 20% will have amputations of the lower limbs in the following 5 years, making DM the
61 leading cause of non-traumatic amputations worldwide (*1*). The resulting treatment costs exceed
62 by far the costs for treating the underlying disease (*2*), underlining the need to develop strategies
63 to prevent these diabetes-related complications.

64 For most complications, it is generally believed that patients with poor glycemic control and longer
65 disease duration are at highest risk. Considering diabetes-related complications of the kidneys,
66 liver, nerves and cardiovascular system, additional risk factors have been identified (*3, 4*). It is
67 assumed that certain anti-diabetic drugs affect bone metabolism and thus influence the fracture
68 risk (*6*). For diabetes-associated complications following orthopedic or trauma surgery,
69 information on risk factors, and consequently treatment recommendations, are yet limited (*5*).

70 In diabetic mice, a massive invasion of neutrophils into wounds was described. Within the
71 wounds, neutrophils were activated to form so-called neutrophil extracellular traps (NETs) (*7*), an
72 unspecific defense mechanism where neutrophils release their DNA together with citrullinated
73 histones and anti-microbial peptides in order to bind and neutralize pathogens (*8*). In wounds of
74 diabetic mice, however, an accumulation of NETs was observed, which impaired the wound
75 healing (*7*), either indirectly by stimulating local inflammation (*9*) or directly by acting as damage-
76 associated molecular patterns harming the surrounding tissue (*10*). These findings in mice have
77 been reproduced in different laboratories ever since (*11-13*). In humans, circulating NETs
78 markers, *e.g.*, neutrophil elastase (ELANE), myeloperoxidase (MPO), citrullinated histones H3
79 (citH3), cell-free (cf) DNA, and nucleosomes, were found to be increased in patients with DM,
80 especially when having foot ulcers (DFUs) - for review see (*14*). The levels of ELANE and citH3

81 were negatively associated with the DFUs' spontaneous healing potential while relating to the
82 amputation rate (*12, 15*). These findings emphasize the important role of NET accumulation for
83 impaired wound healing in patients with DM, and thus provide opportunities for the development
84 of novel treatment strategies. However, when considering that the accumulated NETs may
85 severely damage the surrounding tissue, measuring circulating NET markers may not allow
86 enough time to adjust the treatment in the clinical setting. In order to gain time for treatment a
87 biomarker that indicates the potential of neutrophils to form NETs would be required.
88 Overexpression of peptidyl arginine deiminase 4 (PADI4) in neutrophils was identified to be
89 responsible for the overshooting NET formation in wounds of diabetic mice (*7*). PADI4 is known
90 to convert arginine residues to citrulline in proteins – in case of NETosis mainly in histones,
91 inducing nuclear decondensation (*16*). Even before NETs were first described, a dysregulated
92 PADI4 activity, was related to abnormal citrullination of auto-antibodies in patients with
93 rheumatoid arthritis (RA) - for review see (*17*). The link between PADI4 and onset and progression
94 of RA was strengthened when a genome wide association study identified a RA-associated PADI4
95 haplotype. This PADI4 functional haplotype consists of 3 single nucleotide polymorphisms (SNPs:
96 rs11203366, rs11203367, rs874881), all located on the first 2 exons of the PADI4 gene, resulting
97 in 3 amino acid substitutions in the N-terminal region of the PADI4 enzyme, affecting its structure
98 (*18*). Special about this PADI4 haplotype is its high minor allele frequency, due to which approx.
99 22% of the worldwide population are homozygous for the minor variant (mm; Figure 2A).
100 Recently, other SNPs in the PADI4 gene were proposed as potential risk loci in patients with
101 rheumatoid arthritis, *e.g.*, SNP rs2301888 (*19*), rs2240336, and rs766449 (*20*), however, these
102 SNPs do not belong to the described haplotype ($R^2 < 0.37$, < 0.22, < 0.59, respectively) and failed
103 statistical significance for an European population (*19, 20*), which is the expected majority in this
104 study cohort.
105 Although increased PADI4 activity was associated with excessive NET formation in non-healing
106 diabetics wounds (*14*), no such relationships between the PADI4 haplotype and the healing
107 potential of diabetic wounds or DFUs was shown so far. Based on the mentioned literature it was
108 hypothesized that the PADI4 haplotype influences the neutrophils response to NET-stimuli and
109 that this relates to the clinical outcome of patients with DM undergoing trauma and/or orthopedic

110 surgery. Therefore, this study aimed to investigate the relationship between PADI4 haplotypes,
111 pre-surgical neutrophilic PADI4 expression, and clinical outcomes – specifically delayed wound
112 healing, tissue infections, and delayed bone healing – in patients (with and without diabetes) who
113 underwent surgery at a level 1 trauma center. Additionally, the study sought to determine whether
114 PADI4 haplotypes influence the potential of neutrophils to form NETs.

115 ## Results

116 **Patients with DM have higher complication rates than patients without DM**

117 With the overall aim that the patients without DM fit those with DM regarding age, gender, and
118 BMI, 725 patients qualified for our study. 38 patients were excluded from the study because they
119 refused to participate or blood sampling was not possible. Of the remaining 687 patients, 380
120 were assigned for the control group (without DM) and 307 were assigned for the DM group, based
121 on their medical history, random blood glucose levels, and/or HbA1C values. The clinical data
122 were independently documented by two clinicians without knowing the laboratory data. The
123 development of infections, delayed wound healing, or delayed bone healing following primary
124 interventions was counted as complications. Revision surgeries were counted as complications
125 when fitting into the above defined categories – from these patients PADI4 haplotype was
126 determined but not neutrophilic PADI4 gene expression. Following this classification, the control
127 group contained 245 patients (112 males and 133 females) without complications and 135
128 patients (90 males and 45 females) with complications. Similarly, the DM group contained 112
129 patients (61 males and 51 females) without complications and 195 patients (129 males and 66
130 females) with complications. Interestingly, in the latter there was no significant difference in
131 HbA1C values of patients with (7.8 ± 1.8% / 4.7 – 14.0) and without complications (9.0 ± 3.2% /
132 5.3 – 17.6; Figure 1A). The VENN diagrams show frequent co-occurrence of 2 or 3 of the rated
133 complications, especially in patients with DM (Figure 1B). The age distribution revealed that
134 patients without DM (w/o: 59.4 ± 13.7 years / w/: 57.6 ± 14.9 years) were on average 6 years
135 younger than patients with DM (w/o: 63.5 ± 12.9 years / w/: 64.7 ± 11.4 years), regardless of the
136 occurrence of a complication (Figure 1C). Similarly, the body mass index (BMI) was increased in

137 patients with DM and complications (30.7 ± 6.1 kg/m^2) as compared to the respective controls
138 (28.4 ± 5.8 kg/m^2; Figure 1D). In diabetic mice increased neutrophilic PADI4 expression was
139 associated with impaired wound healing (*7*). Therefore, PADI4 expression was determined in
140 neutrophils, isolated prior to primary surgery. Basal PADI4 expression was significantly increased
141 (1.9 ± 2.5 *vs.* 17.7 ± 45.6; $p < 0.0001$) in neutrophils from patients with DM when compared to
142 matched patients without DM (Figure 1E).

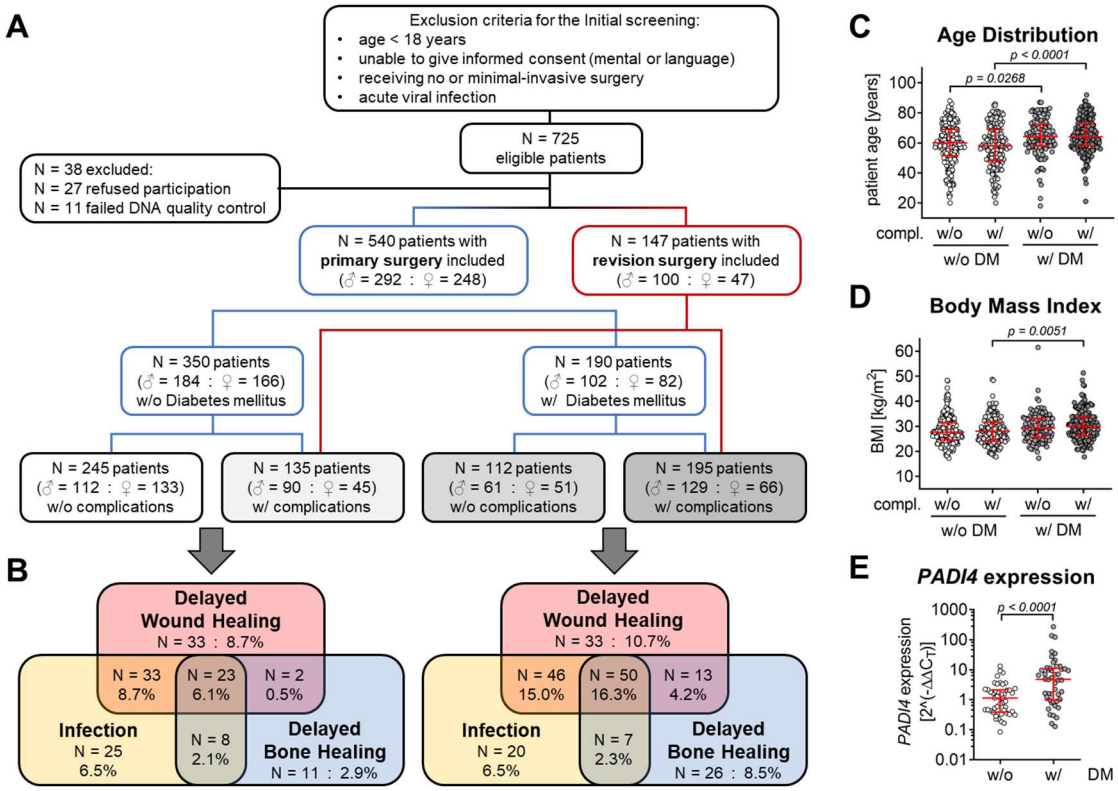

143

144 **Figure 1: Overview on the patients' enrolment in this study.** (A) Patient selection process according to the STREGA
145 guidelines, including patient assignment into the four study groups: patients without diabetes mellitus (Ctrl) and with
146 diabetes mellitus (DM), each with (w/) and without (w/o) complications. Disturbed wound healing, delayed bone healing,
147 and post-surgical infections were counted as complications – when developed within 6 months after a primary
148 intervention. (B) The distribution of the complications is represented as VENN diagrams for patients with and without
149 DM. For each group (C) the patients' age and (D) the individual body mass index (BMI) were obtained. (E) in addition,
150 pre-surgical (primary intervention) PADI4 expression in circulating neutrophils was determined by quantitative real-time
151 PCR in age and gender matched patients (each N = 48). Data are displayed in scatter plots with median and inter-
152 quartile range. Groups were compared by (C&D) ordinary one-way ANOVA followed by Tukey's multiple comparison
153 test or (E) Mann-Whitney test. A $p<0.05$ was considered statistically significant and is shown in the graphs.

154 **PADI4 genotype distribution is independent of the patients' sex, age, BMI, or prevalence**
155 **for diabetes mellitus**

156 All donors were characterized for PADI4 SNPs rs11203366, rs11203367, rs874881 by
157 amplification-refractory mutation system polymerase chain reaction (ARMS-PCR). The haplotype
158 frequency within the study cohort (51.2% A·C·C / 43.1% G·T·G / 5.7% other combinations) was
159 comparable to the reference data available from the 1000 genomes project. Based on these data,

194 patients (28.2%) were identified to be homozygous for the major variant (MM) of PADI4, 116 patients (16.9%) were identified to be homozygous for the minor variant (mm) of PADI4, and the remaining 377 patients (54.9%) were identified to be heterozygous (Mm) of PADI4 (Figure 2A-C). Subgroup analyses revealed, that the PADI4 genotype distribution was independent of the patients' age (Figure 2D), BMI (Figure 2E), sex (Figure 2F), or prevalence for diabetes mellitus (Figure 2G).

PADI4 expression is increased in neutrophils with the PADI4 minor haplotype

A previous report stated that the PADI4 haplotype may affect the mRNA stability (*21*). Therefore, we tested if the basal neutrophilic PADI4 expression levels related to the PADI4 haplotype in our patients. Indeed, neutrophils from patients homozygous for the minor (mm) PADI4 haplotype showed significantly higher PADI4 mRNA levels (4.4 ± 5.5) than neutrophils from patients heterozygous (Mm: 2.0 ± 2.4) or homozygous for the major (MM: 1.1 ± 0.9) PADI4 haplotype (Figure 2H). Due to the high linkage disequilibrium of the three SNPs, similar was observed when investigating the effect of the individual SNPs on basal PADI4 expression levels (data not shown).

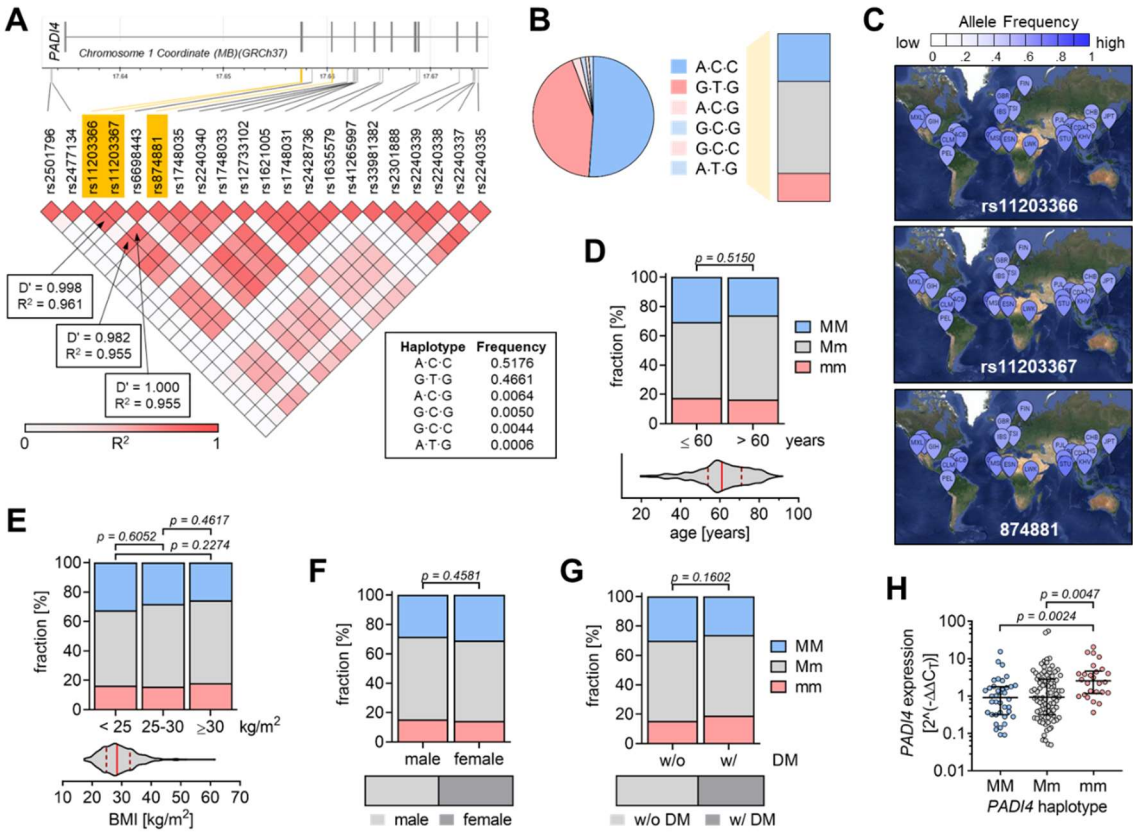

Figure 2: Distribution of the PADI4 haplotype within the study cohort. (A) SNPs within the coding region of the PADI4 gene were retrieved from the Ensemble Genome Browser (https://www.ensembl.org). SNPs with a minor allele frequency > 0·01 were fed into the LDmatrix Tool from the LDlink app (https://www.ldlink.nci.nih.gov). Shown are the

178 obtained D' (deviation of haplotype frequencies from expected values based on gene frequencies) and R^2 (coefficient
179 of determination). The three SNPs with the highest D' and R^2, located within the PADI4 exons, and coding for an amino
180 acid shift were used in this study. The haplotype frequency of these three PADI4 SNPs (rs11203366, rs11203367,
181 rs874881) was determined using the LDhap Tool from the LDlink program. (B) The corresponding PADI4 haplotype
182 frequency of the study cohort was determined by ARMS-PCR. Major and minor haplotype (homozygous) are marked
183 as MM and mm, respectively. Mm: heterozygous. (C) The worldwide allele frequency of the three PADI4 SNPs was
184 determined using the LDpop Tool from the LDlink app. (D) Basal *PADI4* expression in circulating neutrophils (isolated
185 prior to surgery) with different PADI4 haplotypes was determined by quantitative real-time PCR. Data are displayed as
186 scatter plot and groups were compared by nonparametric Kruskal-Wallis test followed by Dunn's multiple comparison
187 test. Haplotype distribution was determined based on the patients' (D) age, (E) body mass index (BMI), (F) sex, or (G)
188 underlying disease (diabetes) and compared by chi-squared (χ^2) test. (H) For all experiments a $p < 0.05$ was considered
189 significant.

190 **Highest PADI4 expression in neutrophils from patients with DM developing complications**

191 As increased neutrophilic PADI4 expression is supposed to affect wound healing (*16*), we related
192 the PADI4 expression levels to the clinical outcome in our patients. PADI4 expression was overall
193 higher in patients with DM when compared to patients without DM. While basal PADI4 expression
194 levels did not significantly differ between patients without DM developing or not a complication,
195 basal PADI4 expression was increased on average by 2.1-fold, 3.7-fold, and 3.1-fold,
196 respectively, in patients with DM developing an infection (Figure 3A), delayed wound healing
197 (DWH / Figure 3B), or delayed bone healing (DBH / Figure 3C). This also displayed in the
198 corresponding receiver operating characteristic (ROC) curves, with areas under the curve (AUC)
199 being significant for patients with DM (Infect: AUC = 0.6748, p = 0.0381 & DWH: AUC = 0.6949,
200 p = 0.0216) but not for those without DM (Infect: AUC = 0.5209, p = 0.7162 & DWH:
201 AUC = 0.5357, p = 0.5603) developing an infection or delayed wound healing (Figure 3D&E). For
202 patients developing delayed bone healing a similar trend (diabetics: AUC = 0.6533, p = 0.1168 &
203 controls: AUC = 0.5318, p = 0.6976) was observed (Figure 3F).

204 **Highest complication rates in patients with DM harboring the PADI4 minor haplotype**

205 Based on the observed relation between neutrophilic PADI4 expression levels and both the PADI4
206 haplotype and the clinical outcome, the PADI4 haplotype was related to the clinical outcome of
207 the patients. Overall, the herein analyzed complications were documented more often in diabetics
208 than controls. In patients without DM, the rate of complications was comparable between patients
209 harboring the major or minor PADI4 haplotype. However, among the patients with DM, those
210 homozygous for the minor PADI4 haplotype developed significantly more infections (mm: 60.7%)
211 than those heterozygous (Mm: 36.5%) or those homozygous for the major (MM: 32.5%) PADI4
212 haplotype (Figure 3G). The same holds for patients with DM and delayed wound healing – the

frequency was highest in those homozygous for the minor PADI4 haplotype (mm: 78.6%), followed by those heterozygous (Mm: 38.8%) or homozygous for the major (MM: 36.3%) PADI4 haplotype (Figure 3H). For patients with DM and delayed bone healing no such trend was observed (Figure 3I). In order to investigate, if a specific pathology associated with delayed bone healing is related to the PADI4 haplotype, a subgroup analysis was performed that differentiated between specific bone-related complication, namely, pseudarthrosis (N = 54), osteomyelitis (N = 39), osteolysis and osteonecrosis (N = 30), independent of the DM-status. Interestingly, in patients with osteomyelitis, osteolysis and osteonecrosis there was an increase in the major PADI4 haplotype as compared to the entire study population. However, with infections present in pseudarthrosis and osteomyelitis, also an increase in minor PADI4 haplotype was observed (Figure 3J).

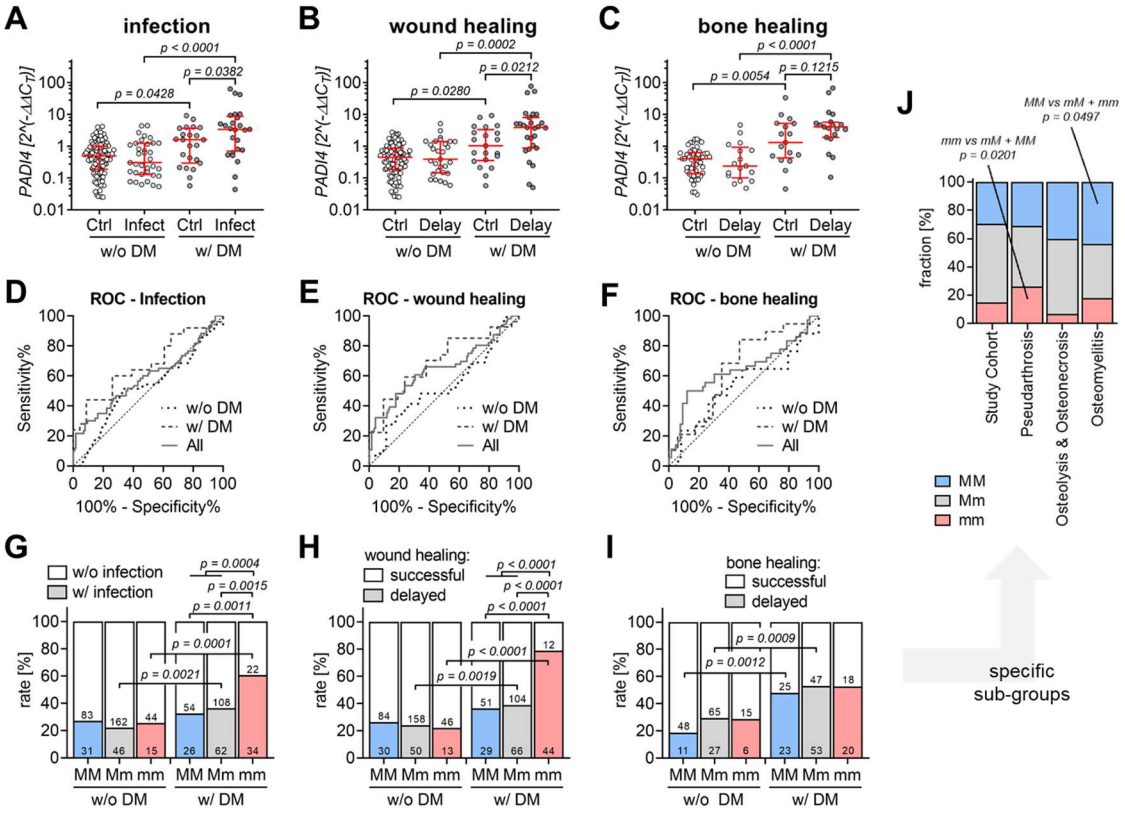

Figure 3: Association of the PADI4 haplotype with PADI4 expression and clinical outcome. (A) PADI4 expression in circulating neutrophils (isolated prior to surgery) was determined by qRT-PCR and related to the three PADI4 SNPs rs11203366, rs11203367, and rs874881, determined by ARMS-PCR. Neutrophilic PADI4 expression was then compared between patients with and without Diabetes mellitus (DM), that did or didn't develop (B) infections, (C) delayed wound healing (DWH), and (D) delayed bone healing (DBH). Data are displayed in scatter plots and groups were compared by nonparametric Kruskal-Wallis test followed by Dunn's multiple comparison test. The PADI4 expression levels were used to generate receiver operating characteristic (ROC) curve for the development of (E) infections, (F) delayed wound healing, and (G) delayed bone healing in control and diabetic patients. PADI4 haplotype distribution based on the patients' underlying disease (controls vs. diabetics) and the clinical outcome, developing (H) infections, (I) delayed wound healing, and (J) delayed bone healing was compared by chi-squared (χ^2) test. For all experiments a $p < 0.05$ was considered significant.

236 Single complication rates attributed to the PADI4 SNPs genotype or allele distribution in patients
237 with and without DM are summarized in Table 1. In line with the PADI4 haplotype distribution the
238 minor alleles of SNPs rs11203366 (A>G), rs11203367 (C>T), and rs874881 (C>G) strongly
239 related to the development of infections and delayed wound healing in patients with DM.
240

241 **Table 1.** Genotype and allele distribution within the study.

		All (N w/o : N w/)			Ctrl (N w/o : N w/)			DM (N w/o : N w/)		
		Infect	**DWH**	**DBH**	**Infect**	**DWH**	**DBH**	**Infect**	**DWH**	**DBH**
rs11203366										
Genotypes	*p-value*	***0.0172***	***0.0005***	*0.0864*	*0.8894*	*0.7976*	*0.1919*	***0.0016***	***<0.0001***	*0.6415*
	AA	131 : 52	128 : 55	70 : 30	78 : 27	78 : 27	45 : 9	53 : 25	50 : 28	25 : 21
	AG	277 : 114	270 : 121	115 : 84	168 : 51	165 : 54	68 : 29	109 : 63	105 : 67	47 : 55
	GG	65 : 48	57 : 56	33 : 26	43 : 14	45 : 12	15 : 6	22 : 34	12 : 44	18 : 20
Alleles	*p-value*	***0.0370***	***0.0047***	*0.0635*	*0.8099*	*0.5767*	*0.1706*	***0.0033***	***<0.0001***	*0.5158*
	A	539 : 218	526 : 231	255 : 144	324 : 105	321 : 108	158 : 47	215 : 113	205 : 123	97 : 97
	G	407 : 210	384 : 233	181 : 136	254 : 79	255 : 78	98 : 41	153 : 131	129 : 155	83 : 95
rs11203367										
Genotypes	*p-value*	***0.0145***	***0.0004***	*0.1119*	*0.6937*	*0.6574*	*0.2789*	***0.0018***	***<0.0001***	*0.8392*
	CC	139 : 57	135 : 61	72 : 32	86 : 31	85 : 32	49 : 11	53 : 26	50 : 29	23 : 21
	CT	268 : 108	262 : 114	112 : 81	159 : 46	157 : 48	64 : 27	109 : 62	105 : 66	48 : 54
	TT	66 : 49	58 : 57	34 : 27	44 : 15	46 : 13	15 : 6	22 : 34	12 : 44	19 : 21
Alleles	*p-value*	***0.0432***	***0.0073***	*0.0683*	*0.7326*	*0.4086*	*0.2066*	***0.0045***	***<0.0001***	*0.6683*
	C	546 : 222	532 : 236	256 : 145	331 : 108	327 : 112	162 : 49	215 : 114	205 : 124	94 : 96
	T	400 : 206	378 : 228	180 : 135	247 : 76	249 : 74	94 : 39	153 : 130	129 : 154	86 : 96
rs874881										
Genotypes	*p-value*	***0.0468***	***0.0009***	*0.2292*	*0.5401*	*0.5879*	*0.3927*	***0.0018***	***<0.0001***	*0.8392*
	CC	125 : 55	123 : 57	68 : 32	77 : 30	77 : 30	45 : 11	48 : 25	46 : 27	23 : 21
	CG	270 : 107	264 : 113	112 : 81	158 : 46	157 : 47	64 : 27	112 : 61	107 : 66	48 : 54
	GG	78 : 52	68 : 62	38 : 27	54 : 16	54 : 16	19 : 6	24 : 36	14 : 46	19 : 21
Alleles	*p-value*	*0.1418*	***0.0123***	*0.1812*	*0.3889*	*0.3998*	*0.4616*	***0.0075***	***<0.0001***	*0.6683*
	C	520 : 217	510 : 227	248 : 145	312 : 106	311 : 107	154 : 49	208 : 111	199 : 120	94 : 96
	G	426 : 211	400 : 237	188 : 135	266 : 78	265 : 79	102 : 39	160 : 133	135 : 158	86 : 96

242 *P-values* are given for the comparison of each MM vs. mm (genotypes) and M vs. m (alleles). Groups were compared
243 by chi-squared (χ^2) test. DWH = delayed wound healing; DBH = delayed bone healing

244 **PADI4 haplotype was associated with PADI4 protein levels and PADI4 activity**

245 As the PADI4 haplotype was related to the PADI4 gene expression levels, we tested their effect
246 on PADI4 protein levels in neutrophils isolated from healthy donors homozygous for the PADI4
247 major or minor haplotype (Figure 4A). Neutrophils with the PADI4 minor haplotype had 2.0-fold
248 higher basal PADI4 levels than neutrophils with the PADI4 major haplotype. As a marker for
249 PADI4 activity the levels of citrullinated histone H3 (cit-H3) were quantified in these cells.
250 Although, basal cit-H3 levels were very low, their levels were 3.5-fold higher in neutrophils with

251 the PADI4 minor haplotype when compared to neutrophils with the PADI4 major haplotype
252 (Figure 4B&C). As additional neutrophil markers protein levels of neutrophil elastase (ELANE)
253 and myeloperoxidase (MPO) were quantified. While ELANE levels were not significantly affected
254 by the PADI4 haplotype, basal MPO levels were 1.7-fold higher in neutrophils with the PADI4
255 major haplotype when compared to neutrophils with the PADI4 minor haplotype (Figure 4D&E).

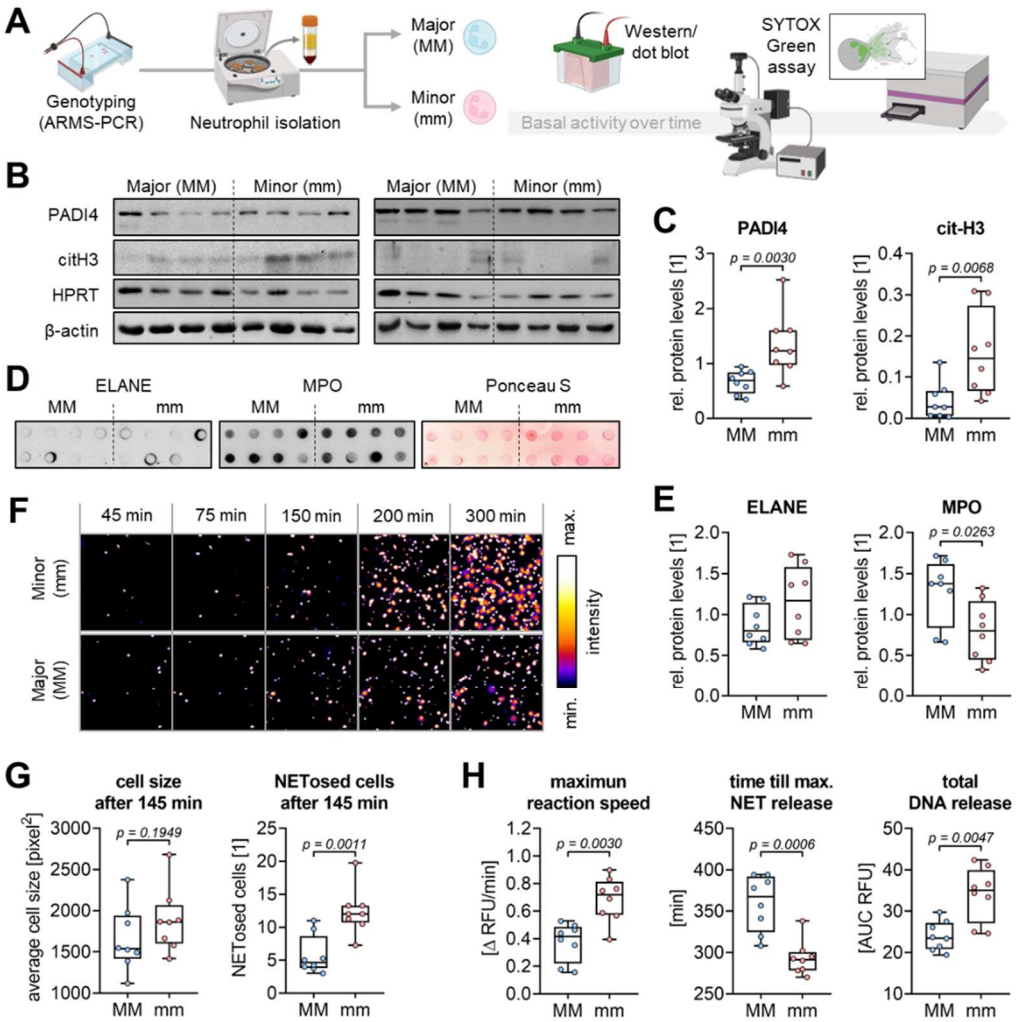

256

257 **Figure 4: Basal NET formation in neutrophils with different PADI4 haplotype.** (A) Schematic overview of the
258 experimental setup – created with icons from BioRender https://www.biorender.com/. Freshly isolated neutrophils from
259 16 healthy donors homozygous for the major (MM: N = 8) or minor (mm: N = 8) PADI4 haplotype were examined for
260 basal neutrophil activation. (B) Western blot images for PADI4 and citrullinated Histone H3 (citH3). (C) Western blot
261 signals for PADI4 and citH3 were quantified by ImageJ software (each membrane with n = 3 exposure times). HPRT
262 and β-actin were used as loading controls. (D) Dot blot images for neutrophil elastase (ELANE) and myeloperoxidase
263 (MPO). (E) Dot blot signals for ELANE and MPO were quantified by ImageJ software (each membrane with n = 3
264 exposure times). Ponceau S staining was used as loading control. (F) Representative time-laps images of the
265 performed SYTOX™ Green Assay. SYTOX™ Green signal intensities were visualized in ImageJ using "fire"
266 pseudocolor. (G) Morphologic analyses (*22*) were performed to detect the average cell size and the number of NETosed
267 cells after 145 min. (H) Curve fitting was done to determine the maximum NET release rate, represented by the
268 strongest increase (slope) in fluorescence, and the time point of maximum NET release, represented by the inflection
269 point of the slope. The total DNA released was determined by the area under the curve (AUC). Data are displayed in
270 box plots with individual data points, median, and interquartile range. Data between two groups were compared by
271 Mann-Whitney U-tests. A $p < 0.05$ was considered significant and is shown in the graphs.

272 **Increased basal NET formation in neutrophils homozygous for the PADI4 minor haplotype**

273 The same neutrophils were analyzed for their potential to form NETs by SYTOX™ Green Assay.
274 Time-laps fluorescent images showed more basal NET formation in neutrophils with the PADI4
275 minor haplotype when compared to neutrophils with the PADI4 major haplotype (Figure 4F).
276 Image analysis confirmed an increased cell size and higher amount of NETosed cells (Figure 4G)
277 145 min after isolation. Fluorescent signals quantified with an Omega plate reader were used for
278 curve fitting. Basal NET formation occurred more rapidly (1.7-fold with Δ 76 min) in neutrophils
279 homozygous for the PADI4 minor haplotype when compared to neutrophils homozygous for the
280 PADI4 major haplotype. Further, neutrophils with the PADI4 minor haplotype released 1.5-fold
281 more DNA than neutrophils with the PADI4 major haplotype (Figure 4H).

282 **PADI4 minor haplotype sensitized neutrophils towards NETosis stimuli**

283 The freshly isolated neutrophils from healthy volunteers homozygous for the PADI4 major or
284 minor haplotype were then stimulated with 100 nM PMA or 4 µM CI, in order to induce NETosis.
285 Within 5 h following stimulation different aspects of NET formation were documented (Figure 5A).
286 Cell attachment and activation were detected by bioimpedance measurement (Figure 5B).
287 Directly after stimulation, the group with the PADI4 minor haplotype showed a more rapid increase
288 in cell index (cell attachment: PMA: 2.0-fold and Δ 17 min; CI: 1.9-fold) than the group with the
289 PADI4 major haplotype. The reaction speed following CI stimulation was so quick that no
290 difference between the two groups could be detected. Later, when NET release predominated,
291 the cell index decreased more rapidly (PMA: 2.8-fold; CI: 1.7-fold) in the group with the PADI4
292 minor haplotype when compared to the group with the PADI4 major haplotype (Figure 5C). As
293 another aspect of NETosis, the DNA release was quantified by SYTOX™ Green Assay
294 (Figure 5D). Neutrophils homozygous for the PADI4 minor haplotype more rapidly released (PMA:
295 1.3-fold with Δ 18 min; CI: 1.7-fold) a larger amount of DNA than neutrophils homozygous for the
296 PADI4 major haplotype (Figure 5E). To verify that necrotic cells did not interfere with the
297 SYTOX™ Green Assay, time-resolved fluorescent images were analyzed. The representative
298 compilation shows, that following stimulation neutrophils with the PADI4 minor haplotype showed
299 more NETosed cells (diffuse fluorescence) than neutrophils with the PADI4 major haplotype.

300 Noteworthy, stimulation with CI induced not only NETosis but also necrosis (condensed
301 fluorescence) in the neutrophils (Figure 5F). Automated image analyses confirmed this
302 observation – in PMA stimulated neutrophils, the average cells size and number of NETosed cells
303 were significantly higher in the group with the PADI4 minor haplotype (1.3-fold and 1.5-fold,
304 respectively) when compared to the group with the PADI4 major haplotype (Figure 5G).

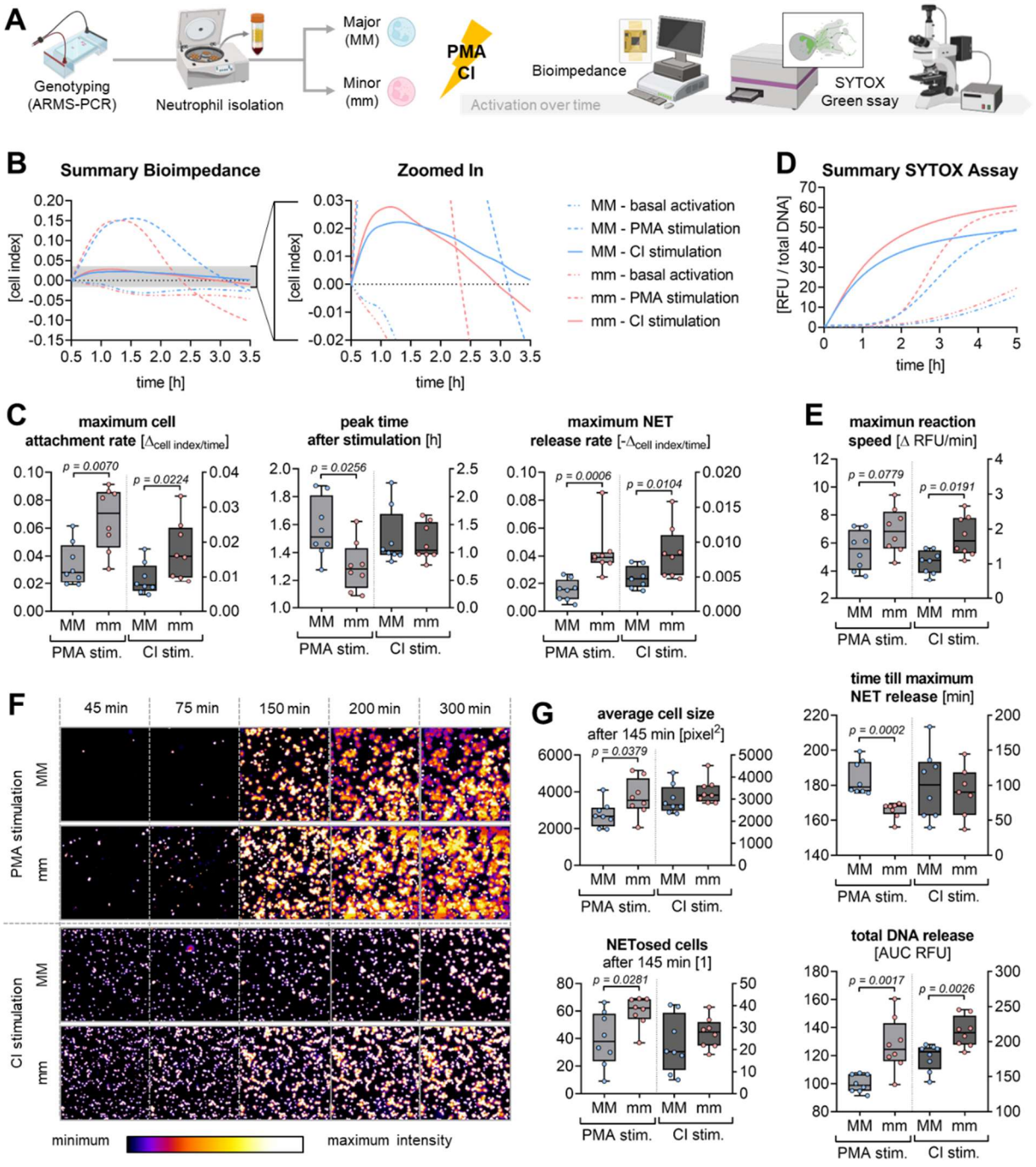

305

306 **Figure 5: PMA- and CI-induced NET formation in neutrophils with different PADI4 haplotype.** (A) Schematic
307 overview of the experimental setup – created with icons from BioRender https://www.biorender.com/. Neutrophils from
308 16 healthy donors homozygous for the major (MM) or minor (mm) PADI4 haplotype were examined for neutrophil
309 activation upon stimulation with 100 nM Phorbol 12-myristate 13-acetate (PMA) or 4 µM calcium ionophore A23187
310 (CI), respectively. Bioimpedance measurement [cell index], using the xCelligence RTCA eSight device, was used to
311 identify early events in neutrophil activation. (A) Curve fitting for the average cell index measured (N = 8, N = 4 per

group). (B) The maximum cell attachment rate was determined by the strongest increase (slope) in cell index. (C) The peak cell index represents the time point when NET release starts to superpose neutrophil attachment. (D) The maximum NET release rate is presented by the strongest decrease (slope) in cell index. In the same cells NET formation / DNA release was quantified by SYTOX™ Green Assay. (E) Curve fitting for the measured fluorescent intensities (N = 8, N = 3 per group). (F) The maximum NET release rate was determined by the strongest increase (slope) in fluorescence. (G) The time point of maximum NET release is represented by the inflection point of the slope. (H) The total DNA released was determined by the area under the curve (AUC). Using the xCelligence RTCA eSight device allowed online detection of fluorescent images from the SYTOX™ Green Assay. (I) Representative time-laps images of the performed SYTOX™ Green Assay with fluorescent intensities visualized in ImageJ using "fire" pseudocolor. Morphologic analyses (*22*) were performed to detect (J) the average cell size and (K) the number of NETosed cells after 145 min. Data are displayed in box plots with individual data points, median, and interquartile range. Data between two groups were compared by Mann-Whitney U-tests. A $p < 0.05$ was considered significant and is shown in the graphs.

Discussion

This study is the first to establish a link between the human PADI4 haplotype (SNPs: rs11203366, rs11203367, rs874881) and wound healing complications in patients with DM undergoing orthopedic and trauma surgery. Furthermore, this functional PADI4 haplotype was linked to neutrophilic PADI4 expression and influenced the neutrophils' ability to form NETs.

Tissue trauma, such as a wound or fracture, leads to release of mitochondrial DNA, which then stimulates neutrophils to form NETs at the site of injury (*23*). Under normal conditions, this is thought to prevent pathogens from colonizing the wound or entering the bloodstream to develop a sepsis. Under diabetic conditions, however, NET accumulation was observed in the wounds, which impaired the healing process (*7*). The resulting increase in circulating NET markers remains even after chronic DFU have developed, and may predict the healing outcome (*12, 15*). In our patients, however, the development of chronic wounds should be prevented. Considering that the accumulated NETs cause damage to the tissue, measuring the amount of NETs formed may not be a suitable approach as it leaves little window of opportunity to adjust treatment. In the diabetic mouse model neutrophilic overexpression of PADI4 was identified as the key inducer for the excessive NET formation (*7*). In line with this, pre-surgical neutrophilic PADI4 levels were significantly increased in our trauma patients with DM, especially in those who later experienced delayed wound healing and/or developed a wound infection. *In vitro*, forced overexpression of PADI4 was reported to induce histone hypercitrullination leading to heterochromatin decondensation and chromatin unfolding (*24*), as well as oxidative burst (*25*), which in case of neutrophils sensitizes the cells for NET stimuli and may even induce spontaneous NET formation.

346 This may explain, why in our experiments both basal and PMA-induced NET formation was
347 increased in neutrophils with increased PADI4 expression.
348 In our patients, pre-surgical PADI4 expression associated not only with the clinical outcome, but
349 also with the investigated PADI4 haplotype – with highest PADI4 expression observed in
350 neutrophils coding for the G T G alleles (minor variant). This is partly in contrast to patients with
351 septic shock, in whom increased PADI4 levels were positively associated to mortality but not with
352 PADI4 SNP rs11203366 (*26*), however, this might be due to the small sample size in the mortality
353 group (N = 41). A study characterizing the PADI4 protein structure proposed, that the base
354 changes in our investigated PADI4 haplotype may alter the PADI4 mRNA stability with prolonged
355 mRNA stability for the minor variant (*21*). This is supporting our findings, that neutrophils with the
356 PADI4 minor haplotype had higher PADI4 mRNA and protein levels. This in turn related with a
357 basal increase in citH3, suggesting that the PADI4 minor haplotype sensitizes neutrophils to
358 release NETs. Indeed, PMA- or CI-induced NET formation was faster and stronger in neutrophils
359 with the PADI4 minor haplotype than in neutrophils with the PADI4 major haplotype.
360 In line with the premise that excessive NET formation in wound tissue is associated with disturbed
361 wound healing in patients with DM, highest PADI4 expression and higher frequency of PADI4
362 minor haplotype was found in neutrophils of patients who later developed a wound healing
363 disorder. Interestingly, the increased complication rate associated with the PADI4 minor
364 haplotype could only be shown in patients with DM, suggesting that DM provides additional NET
365 stimuli. It was proposed that increased glucose levels sensitize neutrophils to form NETs (*27*),
366 more specifically, that exogenous glucose and glycolysis promotes the actual NET release but
367 not the initial chromatin decondensation (*28*). Another study proposed that hyperglycemia
368 supports just the latter by nuclear accumulation of acetyl-CoA, which acts as substrate for histone
369 acetyltransferases (*29*). Yet another study suggested that not the glucose itself, but increased
370 homocysteine levels in DM are the actual trigger for NET formation (*30*). It is questionable if both
371 factors can be discussed independently, as homocysteine levels are positively associated with
372 insulin resistance, dyslipidemia, and poor glucose control (*31*). Both have in common that they
373 induce cellular stress, which increases intracellular calcium levels, a process involving
374 gasdermine E (*32, 33*). The increase in intracellular calcium may than act as a co-factor for the

375 PADI4 enzyme (*34*), but also independently stimulate NET formation as observed for stimulation
376 with calcium-ionophore (*35*).
377 Hyperglycemia is well recognized as a normal metabolic stress response. Therefore, it should be
378 considered that our study cohort consists of trauma patients. In such patients' blood glucose
379 control is aggravated by the stress induced by a trauma and following surgery, resulting in
380 frequent hyperglycemic episodes (*36*). The resulting elevation in basal PADI4 expression might
381 explain, why NET markers are stronger increased in patients with DM following trauma, but also
382 offers the opportunity for an intensified blood glucose control upon hospital admission. First hints
383 are provided from studies with critically-ill patients (ΣN > 7,000) in the intensive care unit (ICU)
384 (*37, 38*). In these patients, strict blood glucose control by intensified insulin treatment (IIT) reduced
385 morbidity and mortality, with the consequence of faster weaning of the mechanical ventilation,
386 discharge from the ICU and hospital. However, a subgroup analysis showed that only trauma
387 patients and patients receiving corticosteroid therapy may have an advantage in survival upon IIT
388 (*40*). Furthermore, strict glycemic control was shown to significantly reduce (50-60%) the
389 incidence of nosocomial infections in surgical ICU patients (*39*).
390 Our data clearly link the PADI4 haplotype with the neutrophilic PADI4 expression in humans,
391 which in turn sensitizes the cells to form NETs. Therefore, genotyping for the PADI4 haplotype
392 might become a relevant screening tool in the future, not only to identify patients with DM at
393 increased risk of developing wound healing disorders but also for other pathologies, *e.g.*, RA,
394 sepsis, deep vein thrombosis, multiple sclerosis, *etc.*, where excessive NET formation and more
395 precisely dysregulated PADI4 activity has been shown to aggravate disease progression (*16*).
396 This is of special importance as such a haplotype screening can be done at the initial diagnosis
397 of the disease, which allows for early intervention. Considering the pathologic role of excessive
398 NET formation could identify novel therapeutic options for such diseases, *e.g.*, enzymatic
399 digestion of he formed NETs (*7*) or ir-/reversible PADI4 inhibitors, *e.g.*, GSK199, GSK484, TDCA,
400 TDFA, JBI-589, F- or Cl-amidine (*34, 41*). However, treatment strategies should involve
401 suppression of excessive NET formation not total depletion of NETs, as this might increase the
402 risk for infections and sepsis (*42, 43*).

403 ## Conclusion

404 In summary, we here provide first evidence that the PADI4 genetic variation influences neutrophil
405 behavior and clinical outcomes. The PADI4 minor haplotype sensitized neutrophils toward NET
406 formation and was associated with an increased complication rate in patients with DM following
407 orthopedic or trauma surgery. PADI4 haplotyping may provide a clinically actionable biomarker to
408 identify patients with DM at high risk for wound healing and infectious complications early upon
409 hospital admission, enabling closer monitoring and/or personalized treatment to prevent
410 complications.

411 ## Methods

412 **Study cohort and sampling**

413 Between September 2018 and February 2022, 687 patients were included in the study by giving
414 their written informed consent (666/2018BO2). During recruitment there was no discrimination by
415 sex, resulting in a sex distribution of 57.1% males (N = 392) and 42.9% females (N = 295). From
416 each individual, swabs of the mucous membrane or EDTA-venous blood were collected.
417 Information about the clinical outcome was independently collected by two physicians in a blinded
418 manner. Disturbed wound healing, delayed bone healing, and post-surgical infections were rated
419 as complications, both as result of a surgery or as cause for a revision surgery. Noteworthy, bone
420 healing was not considered in patients receiving a total joint arthroplasty. Clinical data were
421 merged with the laboratory data only when data acquisition was finished and verified by a second
422 investigator.

423 **Isolation of neutrophils**

424 Neutrophils were isolated from EDTA-venous blood by density gradient centrifugation, as
425 described in (*44*). Isolated neutrophils were quantified by Trypan Blue exclusion method, then
426 diluted to obtain a density of 1 Mio neutrophils/mL (concentrated cell suspension).

427 **qRT-PCR**

428 Total mRNA from freshly isolated neutrophils was isolated by phenol-chloroform extraction and
429 photometrically quantified. Total mRNA was converted into cDNA using the first-strand cDNA

430 synthesis kit (ThermoFisher Scientific, Sindelfingen, GER). Quantitative RT-PCRs were
431 performed using the Green Master Mix (2X) High Rox (Biozym, Hessisch Oldendorf, GER) and
432 the StepOnePlus™ qPCR cycler. Specificity of the qPCR reactions was checked by melting curve
433 analyses. Relative PADI4 expression levels were calculated using the $\Delta\Delta C_T$ method, normalized
434 to *EF1α* and *RPL13a*, which proved to be most stable (GeNorm, NormFinder, Best Keeper,
435 comparative ΔCt method) between individuals (*45*). PCR conditions are summarized in Table 2.

436 **Table 2.** Detailed information on primers (designed with primer blast) and the corresponding optimized qPCR
437 conditions.

Target	GenID	Primer	efficiency	Amplicon	T_A
EF1α	NM_001402.5	For-CCCCGACACAGTAGCATTTG Rev-TGACTTTCCATCCCTTGAACC	1.90	98 bp	56°C
RPL13a	NM_012423.3	For-AAGTACCAGGCAGTGACAG Rev-CCTGTTTCCGTAGCCTCATG	2.24	100 bp	56°C
PADI4	NM_012387.2	For-AGAGGTGACCCTGACGATGA Rev-CAGGTCTTCGCTGTCAAGCA	2.09	310 bp	56°C

438 **Amplification Refractory Mutation System (ARMS) PCR**

439 DNA was isolated from residual leukocytes obtained from neutrophil isolation or swabs of the
440 mucous membrane, as described in (*46*). SNPs were characterized by ARMS-PCR (*46*), using
441 3 µL of DNA (50-100 ng/µL), a mix of 4 primers (Table 3), and the Red HS Taq (2X) Master Mix
442 (Biozym). The amplified DNA was separated by electrophoresis using a 2% agarose gel and
443 visualized with ethidium bromide.

444 **Table 3.** Primer sequences and ARMS-PCR conditions

SNP	primer	primer sequence (5' - 3')	amplicons			T_a
			flanking	allele specific		
rs11203366	IFP	AGGGGTGGTCGTGGATATTGCCCCCA	-	} 179 bp	G-allele (m)	64°C
	ORP	AGCTCTTCCACAGGGCAAGAGGCTCTGC	} 382 bp			
	OFP	AGGAGAAATGCTGGGAGAGCCATGGCT		} 258 bp	A-allele (M)	
	IRP	CCTGTGGATTTCTTCTTGGCTGGAGGTCC	-			
rs11203367	IFP	GGGTAGAGGTGACCCTGACGATGAACGC	-	} 168 bp	T-allele (m)	68°C
	ORP	TGACCTCCATGAACCCCTGGTAGCCGTA	} 364 bp			
	OFP	GAGGACTGCACGTCCTTCAGCATCAACG		} 250 bp	C-allele (M)	
	IRP	CTGGTCGCCTGTGCTACCACTGGACA	-			
rs874881	IFP	CAAAGCTCTACTCTACCTCACGGG	-	} 183 bp	G-allele (m)	62°C
	ORP	ACTCCCAGATGTCTGACTGGCT	} 387 bp			
	OFP	GCTTTCCCTCCATTCCCATC		} 248 bp	C-allele (M)	
	IRP	TGGTTGTCACTTACCCAGCG	-			

445 Primers were designed using a program developed by Ye (http://primer1.soton.ac.uk/primer1.html) (*47*) and
446 synthesized by Eurofins Genomics (Ebersberg, Germany). IFP: inner forward primer, ORP: outer reverse primer, OFP:
447 outer forward primer, IRP: inner reverse primer

448 **Western blot and dot blot**

449 Neutrophils were lyzed with ice-cold RIPA buffer with protease- and phosphatase inhibitors. For
450 Western blot 35 µg total protein was separated by SDS-PAGE and transferred to nitrocellulose
451 membranes. For dot blot 35 µg total protein was directly applied to nitrocellulose membranes
452 under vacuum using a dot blotter (Carl Roth, Karlsruhe, GER). Protein transfer to membraned
453 was confirmed by Ponceau S staining. Unspecific binding sites were blocked with 5% BSA for
454 1 h. After overnight incubation with primary antibodies at +4°C (PADI4: sc-365369, HPRT: sc-
455 376938, ELANE: sc-55548, MPO: sc-52707 - SantaCruz Biotechnology, Heidelberg, GER); Cit-
456 H3: ab5103 (abcam, Cambridge, GBR); β-Actin: #4970 (Cell Signaling Technology, Danver, MA,
457 USA)), membranes were incubated with the corresponding peroxidase-labeled secondary
458 antibodies for 2 h. Enhanced chemiluminescence solution was added and the resulting signals
459 were detected with a CCD camera and quantified with ImageJ.

460 **Stimulation of neutrophils**

461 For all functional assays, neutrophils were stimulated with PMA (Phorbol 12-myristate 13-acetate)
462 or calcium ionophore A23187 (CI). Solutions were prepared as 1.25-fold of the final concentration
463 to allow measurement of blank (80 µL) and thereafter addition of concentrated cell suspension
464 (20 µL) to receive a final concentration of $2*10^5$ neutrophils/mL (*44*).

465 **SYTOX™ Green Assay**

466 1.25 µM SYTOX™ Green was added to the stimulation solutions before the addition of
467 neutrophils. Cells were lysed with 1% Triton-X-100 (Carl Roth, Karlsruhe, Germany) for
468 normalization and better comparability of donors. Fluorescence (λ_{ex}=485 nm & λ_{em}=520 nm) was
469 measured every 30 min with the Omega Plate Reader (BMG Lab-tech) at 37°C and 5% CO_2.
470 Curve fitting of the resulting XY diagrams with GraphPad Prism included; (1) the maximum slope,
471 which equals the maximum NET release rate; (2) the inflection point of the slope, which defines
472 the time till maximum NET release; and (3) the area under the curve (AUC), which represents the
473 total DNA released (*44*).

474 **Bioimpedance measurements and real-time fluorescent imaging**

475 The xCelligence RTCA eSight device (Omni Life Sciences), placed in an incubator at 37°C with
476 5% CO_2 and humidified atmosphere, was used to measure bioimpedance [cell index] (*44*).
477 Neutrophils were stimulated in xCelligence measurement plates containing SYTOX™ Green for
478 real-time fluorescent imaging. After blank measurements, neutrophils were added and cell index
479 was measured at least every 15 min for a period of 6 h. Fluorescence pictures were captured at
480 least every 30 min. Curve fitting of the exported normalized data with GraphPad Prism included;
481 (1) the maximum positive slope, which equals the maximum cell attachment rate; (2) the peak
482 time after stimulation, which represents the time point when cell attachment and NET release are
483 balanced; and (3) the minimum negative slope, which represents the maximum NET release rate.
484 Real-time fluorescent images were exported as single tiff images and compiled in ImageJ:
485 SYTOX™ Green signal intensities were visualized in "fire" pseudocolor. Images of the 145 min
486 time point (one image per well of the GFP channel) were subjected to automatic counting
487 (particles >1,000 $pixel^2$), using an auto local threshold (Bernsen, radius 30) and watershed
488 separation on the respective binary images.

489 **Statistics**

490 Patient data are displayed in violin plots, visually confirming a Gaussian distribution (skewness
491 and kurtosis between -1 and 1). Data comparison was done by ordinary one-way ANOVA followed
492 by Tukey's multiple comparison test. Complication rates in the different groups were compared
493 by chi-squared (χ^2) test. *In vitro* experiments were performed with neutrophils from 8 donors per
494 group (N = 8) with at least three technical replicates ($n \geq 3$). Data are represented as box plots
495 with individual measurement points, median, and interquartile range. Given the smaller sample
496 size, Gaussian distribution cannot be assumed for the *in vitro* experiments, thus, data were
497 compared by Mann-Whitney U-tests. For all experiments a $p < 0.05$ was considered significant.
498 GraphPad Prism 8.0.1 was used to perform statistical analysis and generate graphs.

499 **Study approval**

500 The study was approved by the ethics committee of the University Hospital Tübingen (ethical vote
501 666/2018BO2, approved 20.09.2018).

Data availability: All data supporting the findings of this study are available within the paper. The anonymized dataset generated and analyzed during the current study are fully available without restriction from the corresponding author.

Author contributions: S.E. – conceptualization of the study; funding acquisition; methodology and investigations; formal analysis and validation of the laboratory data; data visualization; writing of the manuscript draft. P.H. & C.I. – patient recruitment and retrieval of patient data; validation of the clinical (trauma) data. C.L. & J.M. – methodology and investigations. P.-G.A. & R.L. – resources and patient data; validation of the clinical (diabetes) data. G.B. – statistic counseling. S.P. & A.F. – recourses, validation of the clinical (diabetes) data. H.B., M.F.R. & T.H. – resources and patient data. A.K.N. – resources; supervision; validation of the laboratory data. All authors have reviewed and edited the manuscript and agreed to its published version.

References

1. S. Pscherer, F. W. Dippel, S. Lauterbach, K. Kostev, Amputation rate and risk factors in type 2 patients with diabetic foot syndrome under real-life conditions in Germany. *Prim Care Diabetes* **6**, 241-246 (2012).
2. I. Koster, L. von Ferber, P. Ihle, I. Schubert, H. Hauner, The cost burden of diabetes mellitus: the evidence from Germany--the CoDiM study. *Diabetologia* **49**, 1498-1504 (2006).
3. O. P. Zaharia *et al.*, Risk of diabetes-associated diseases in subgroups of patients with recent-onset diabetes: a 5-year follow-up study. *Lancet Diabetes Endocrinol* **7**, 684-694 (2019).
4. E. Ahlqvist *et al.*, Novel subgroups of adult-onset diabetes and their association with outcomes: a data-driven cluster analysis of six variables. *Lancet Diabetes Endocrinol* **6**, 361-369 (2018).
5. Y. Chen, Y. Zhou, J. Lin, S. Zhang, Challenges to Improve Bone Healing Under Diabetic Conditions. *Front Endocrinol (Lausanne)* **13**, 861878 (2022).

528 6. Y. S. Zhang, Y. D. Zheng, Y. Yuan, S. C. Chen, B. C. Xie, Effects of Anti-Diabetic Drugs
529 on Fracture Risk: A Systematic Review and Network Meta-Analysis. *Front Endocrinol*
530 *(Lausanne)*, 735824 (2021).
531 7. S. L. Wong *et al.*, Diabetes primes neutrophils to undergo NETosis, which impairs wound
532 healing. *Nat Med* **21**, 815-819 (2015).
533 8. V. Brinkmann *et al.*, Neutrophil extracellular traps kill bacteria. *Science* **303**, 1532-1535
534 (2004).
535 9. S. Zhu *et al.*, The emerging roles of neutrophil extracellular traps in wound healing. *Cell*
536 *Death Dis* **12**, 984 (2021).
537 10. N. L. Denning, M. Aziz, S. D. Gurien, P. Wang, DAMPs and NETs in Sepsis. *Front*
538 *Immunol* **10**, 2536 (2019).
539 11. L. Menegazzo *et al.*, The antidiabetic drug metformin blunts NETosis in vitro and reduces
540 circulating NETosis biomarkers in vivo. *Acta Diabetol* **55**, 593-601 (2018).
541 12. G. P. Fadini *et al.*, NETosis Delays Diabetic Wound Healing in Mice and Humans.
542 *Diabetes* **65**, 1061-1071 (2016).
543 13. S. K. Das, Y. F. Yuan, M. Q. Li, Specific PKC betaII inhibitor: one stone two birds in the
544 treatment of diabetic foot ulcers. *Biosci Rep* **38**, (2018).
545 14. R. Njeim *et al.*, NETosis contributes to the pathogenesis of diabetes and its complications.
546 *J Mol Endocrinol* **65**, R65-R76 (2020).
547 15. S. Yang *et al.*, Neutrophil Extracellular Traps Are Markers of Wound Healing Impairment
548 in Patients with Diabetic Foot Ulcers Treated in a Multidisciplinary Setting. *Adv Wound*
549 *Care (New Rochelle)* **9**, 16-27 (2020).
550 16. S. L. Wong, D. D. Wagner, Peptidylarginine deiminase 4: a nuclear button triggering
551 neutrophil extracellular traps in inflammatory diseases and aging. *FASEB J*, fj201800691R
552 (2018).
553 17. J. E. Jones, C. P. Causey, B. Knuckley, J. L. Slack-Noyes, P. R. Thompson, Protein
554 arginine deiminase 4 (PAD4): Current understanding and future therapeutic potential. *Curr*
555 *Opin Drug Discov Devel* **12**, 616-627 (2009).

556 18. A. Suzuki *et al.*, Functional haplotypes of PADI4, encoding citrullinating enzyme
557 peptidylarginine deiminase 4, are associated with rheumatoid arthritis. *Nat Genet* **34**, 395-
558 402 (2003).
559 19. Y. Okada *et al.*, Genetics of rheumatoid arthritis contributes to biology and drug discovery.
560 *Nature* **506**, 376-381 (2014).
561 20. S. Eyre *et al.*, High-density genetic mapping identifies new susceptibility loci for
562 rheumatoid arthritis. *Nat Genet* **44**, 1336-1340 (2012).
563 21. N. Horikoshi *et al.*, Structural and biochemical analyses of the human PAD4 variant
564 encoded by a functional haplotype gene. *Acta Crystallogr D Biol Crystallogr* **67**, 112-118
565 (2011).
566 22. V. Brinkmann, C. Goosmann, L. I. Kuhn, A. Zychlinsky, Automatic quantification of in vitro
567 NET formation. *Front Immunol* **3**, 413 (2012).
568 23. K. Itagaki *et al.*, Mitochondrial DNA released by trauma induces neutrophil extracellular
569 traps. *PLoS One* **10**, e0120549 (2015).
570 24. M. Leshner *et al.*, PAD4 mediated histone hypercitrullination induces heterochromatin
571 decondensation and chromatin unfolding to form neutrophil extracellular trap-like
572 structures. *Front Immunol* **3**, 307 (2012).
573 25. Y. Zhou *et al.*, Evidence for a direct link between PAD4-mediated citrullination and the
574 oxidative burst in human neutrophils. *Sci Rep* **8**, 15228 (2018).
575 26. N. A. Costa *et al.*, Peptidylarginine deiminase 4 concentration, but not PADI4
576 polymorphisms, is associated with ICU mortality in septic shock patients. *J Cell Mol Med*
577 **22**, 4732-4737 (2018).
578 27. L. Menegazzo *et al.*, NETosis is induced by high glucose and associated with type 2
579 diabetes. *Acta Diabetol* **52**, 497-503 (2015).
580 28. O. Rodriguez-Espinosa, O. Rojas-Espinosa, M. M. Moreno-Altamirano, E. O. Lopez-
581 Villegas, F. J. Sanchez-Garcia, Metabolic requirements for neutrophil extracellular traps
582 formation. *Immunology* **145**, 213-224 (2015).
583 29. S. Shrestha *et al.*, Diabetes Primes Neutrophils for Neutrophil Extracellular Trap
584 Formation through Trained Immunity. *Research (Wash D C)* **7**, 0365 (2024).

585 30. M. B. Joshi *et al.*, Elevated homocysteine levels in type 2 diabetes induce constitutive
586 neutrophil extracellular traps. *Sci Rep* **6**, 36362 (2016).
587 31. X. Zhang *et al.*, Homocysteine inhibits pro-insulin receptor cleavage and causes insulin
588 resistance via protein cysteine-homocysteinylation. *Cell Rep* **37**, 109821 (2021).
589 32. S. Koushik *et al.*, PAD4: pathophysiology, current therapeutics and future perspective in
590 rheumatoid arthritis. *Expert Opin Ther Targets* **21**, 433-447 (2017).
591 33. D. N. Douda, M. A. Khan, H. Grasemann, N. Palaniyar, SK3 channel and mitochondrial
592 ROS mediate NADPH oxidase-independent NETosis induced by calcium influx. *Proc Natl*
593 *Acad Sci U S A* **112**, 2817-2822 (2015).
594 34. F. Ma *et al.*, Gasdermin E dictates inflammatory responses by controlling the mode of
595 neutrophil death. *Nat Commun* **15**, 386 (2024).
596 35. Y. P. Zhu *et al.*, NET formation is a default epigenetic program controlled by PAD4 in
597 apoptotic neutrophils. *Sci Adv* **9**, eadj1397 (2023).
598 36. P. L. Bosarge, J. D. Kerby, Stress-induced hyperglycemia: is it harmful following trauma?
599 *Adv Surg* **47**, 287-297 (2013).
600 37. G. Van den Berghe *et al.*, Intensive insulin therapy in the medical ICU. *N Engl J Med* **354**,
601 449-461 (2006).
602 38. G. van den Berghe *et al.*, Intensive insulin therapy in critically ill patients. *N Engl J Med*
603 **345**, 1359-1367 (2001).
604 39. N. J. Grey, G. A. Perdrizet, Reduction of nosocomial infections in the surgical intensive-
605 care unit by strict glycemic control. *Endocr Pract* **10 Suppl 2**, 46-52 (2004).
606 40. N.-S. S. Investigators *et al.*, Intensive versus conventional glucose control in critically ill
607 patients. *N Engl J Med* **360**, 1283-1297 (2009).
608 41. C. Gajendran *et al.*, Alleviation of arthritis through prevention of neutrophil extracellular
609 traps by an orally available inhibitor of protein arginine deiminase 4. *Scientific reports* **13**,
610 3189 (2023).
611 42. W. Meng *et al.*, Depletion of neutrophil extracellular traps in vivo results in
612 hypersusceptibility to polymicrobial sepsis in mice. *Crit Care* **16**, R137 (2012).

613 43. A. P. Stewart *et al.*, Neutrophil extracellular traps protect the kidney from ascending
614 infection and are required for a positive leukocyte dipstick test. *Sci Transl Med* **16**,
615 eadh5090 (2024).
616 44. C. Linnemann, S. Venturelli, F. Konrad, A. K. Nussler, S. Ehnert, Bio-Impedance
617 measurement allows displaying the early stages of Neutrophil Extracellular Traps. *EXCLI*
618 *Journal* **19**, 1481-1495 (2020).
619 45. R. H. Aspera-Werz *et al.*, Nicotine and Cotinine Induce Neutrophil Extracellular Trap
620 Formation-Potential Risk for Impaired Wound Healing in Smokers. *Antioxidants (Basel)*
621 **11**, (2022).
622 46. S. Ehnert *et al.*, One-Step ARMS-PCR for the Detection of SNPs-Using the Example of
623 the PADI4 Gene. *Methods Protoc* **2**, (2019).
624 47. S. Ye, S. Dhillon, X. Ke, A. R. Collins, I. N. Day, An efficient procedure for genotyping
625 single nucleotide polymorphisms. *Nucleic Acids Res* **29**, E88-88 (2001).